Neuropsychiatric Disease and Treatment

Dovepress

open access to scientific and medical research

Open Access Full Text Article

ORIGINAL RESEARCH

Investigation of Changes in Retinal Detachment-Related Brain Region Activities and Functions Using the Percent Amplitude of Fluctuation Method: A Resting-State Functional Magnetic Resonance Imaging Study

This article was published in the following Dove Press journal:
Neuropsychiatric Disease and Treatment

Yan-Chang Yang[1,*]
Qiu-Yu Li[2,*]
Min-Jie Chen[2]
Li-Juan Zhang[2]
Meng-Yao Zhang[1]
Yi-Cong Pan[2]
Qian-Min Ge[2]
Hui-Ye Shu[2]
Qi Lin[2]
Yi Shao[2]

[1]Department of Ophthalmology, Nanchang University, Jiangxi Province Clinical Ophthalmology Institute, Nanchang 330006, Jiangxi, People's Republic of China; [2]Department of Ophthalmology, The First Affiliated Hospital of Nanchang University, Jiangxi Province Clinical Ophthalmology Institute, Nanchang 330006, Jiangxi, People's Republic of China

*These authors contributed equally to this work

Purpose: The percent amplitude of fluctuation (PerAF) method was used to study the changes in neural activities and functions in specific brain regions of patients with a retinal detachment (RD).

Patients and Methods: In this study, we recruited 15 RD patients (nine males and six females) and 15 healthy controls (HCs) matched for gender, age, and weight. All participants were scanned with resting functional magnetic resonance imaging (rs-fMRI). The PerAF method was then used for data analysis to evaluate and detect changes in neural activity in relevant brain regions. Receiver operating characteristic (ROC) curve analysis was used to evaluate the two groups.

Results: The PerAF signal values of the right fusiform gyrus and the left inferior temporal gyrus of RD patients were significantly higher than those of HCs. This may indicate changes in neural activity and function in the related brain regions. The anxiety and depression scores of hospital anxiety and depression scale (HADS) and the durations in RD patients were positively correlated with the PerAF values of the left inferior temporal gyrus.

Conclusion: In this study, we demonstrated that there were significant changes in the PerAF values in specific areas of the brain in patients with RD. The change of PerAF values represent the changes of BOLD signal intensity, which reflect the hyperactivity or weakening of specific brain regions in RD patients, which are helpful to predict the development and prognosis of RD patients, and play an important role in the early diagnosis of RD. In addition, according to the results, changes in neural activity in specific brain regions of RD patients increase the risk of brain dysfunction related diseases, which may help to understand the pathological mechanism of vision loss in RD patients.

Keywords: retinal detachment, the percent amplitude of fluctuation, resting-state, functional magnetic resonance imaging, hospital anxiety and depression scale

Correspondence: Yi Shao
Department of Ophthalmology, The First Affiliated Hospital of Nanchang University, Jiangxi Province Clinical Ophthalmology Institute, 17 Yongwaizheng Street, Donghu, Nanchang, Jiangxi 330006, People's Republic of China
Email freebee99@163.com

Introduction

Retinal detachment (RD) is a dreaded eye disease. Maintaining a direct connection between the retina and retinal pigment epithelium is the basis for retinal function. When RD occurs in the fovea, it can lead to severe loss of vision and even blindness.[1] There are many circumstances that lead to RD and rhegmatogenous

RD is the most common type. It is mainly due to retinal fissure or tearing so that liquid enters and accumulates under the retina to separate the retina from the block below.[2] In addition, mechanical traction and fluid exudation can cause the disease.[3] Patients with RD have obvious visual abnormalities, which are characterized by "flying mosquito syndrome," blurred or defective visual field, abnormal light spots, visual loss, and even blindness within hours or days.[4] At present, surgery is the most commonly used method for the treatment of RD.[5]

Ultrasound is one of the effective methods for the diagnosis of RD, with a sensitivity of 94.2%,[6] but it cannot be used to determine the range, severity, and microscopic changes in the retina. SD-OCT is also an effective method for analyzing and diagnosing changes in the retinal layer in RD. This technology can be used to accurately evaluate the structure of different retinal layers and the optic nerve.[7] However, there has been no report on changes in the visual center in patients with RD, and the related neural mechanism is not clear. The using of imaging techniques to determine the structure and function of specific brain regions, especially the visual pathway, can help with exploration of the pathogenesis of RD, and early diagnosis and prognosis can also benefit treatment of RD.

At present, task-based fMRI is a technology used to evaluate and analyze the functional and structural changes in the human brain. Rs-fMRI has been used to analyze brain functional areas compared with other types of fMRI because it is easy to obtain signals, requires a minimum workload from patients, and has proficiency in identifying functional areas of the brain.[8] In recent years, many studies have used the amplitude of low-frequency fluctuations (ALFF) method to describe the activity intensity of an individual element in space by measuring spontaneous fluctuation in the process of brain nerve activity to study changes in various brain activities.[9] However, due to the arbitrary unit of BOLD signals, subsequent statistical analysis is difficult. Regional homogeneity (ReHo) is a newly developed method that can be used to evaluate the similarity or consistency of spontaneous low-frequency (<0.08 Hz) BOLD signal fluctuations in whole-brain voxel analysis. However, since it is based on time consistency, it can analyze the brain functional state as a whole, but it cannot reflect the activity of neurons in a certain integrin.[10] At present, many studies have proposed the percent amplitude of fluctuation (PerAF) of re-fMRI using the percentage of signal changes in a task functional MRI.[11] Although rs-fMRI lacks a clear control design, the percentage of BOLD signal intensities relative to the average BOLD signal intensity at each time point is measured and the average value is obtained in the whole time series, which is the "percent amplitude of fluctuation" or PerAF.[12] PerAF could be further standardized by global mean PerAF, ie, mPerAF. The mPerAF has two stages of standardization, the first is the percentage of fluctuation amplitude at the single voxel or signal time series level. The second is divided by the average PerAF of the whole brain. In other words, mPerAF can correct the change caused by the difference of relative BOLD signal strength.[12] Some studies have shown that PerAF shows similar scanner internal reliability as ALFF, but with reduced influence of the BOLD signal strength, and it can become a higher reliability index than ALFF, ReHo, and degree centrality (DC).[11] Therefore, PerAF has great potential in voxel whole-brain analysis. Unfortunately, there are few studies that have used PerAF to explore the characteristic changes in brain function and activity.

This is the first study assessing the changes in neural activity and brain function in patients with RD using the PerAF method, which may provide a basis for an early diagnosis and prognosis of patients with RD.

Patients and Methods

Participants

We enrolled 15 patients with RD from the Ophthalmology Department of the First Affiliated Hospital of Nanchang University, including nine males and six females. The selection criteria for the RD group were: (1) age 20~60 years old; (2) idiopathic RD with 1−2 retinal tears detected by ophthalmic ultrasound; (3) RD range not exceeding two quadrants; and (4) no other ophthalmic diseases (eg, optic neuritis and glaucoma). The exclusion criteria of the RD group were: (1) patients with RD who had received eye surgery or laser therapy; (2) RD patients with severe complications (such as macular degeneration and vitreous hemorrhage); (3) patients with RD secondary to ocular trauma; and (4) RD patients with other systemic diseases. An example of RD seen by ocular ultrasound is shown in Figure 1.

Fifteen healthy controls (HCS; nine males and six females) were included in the study, and they were closely matched in gender, age, and weight with the RD group. The HC group met the following conditions: (1) patients with uncorrected visual acuity > 1.0; (2) could accept MRI scanning (such as no pacemaker or other implanted metal

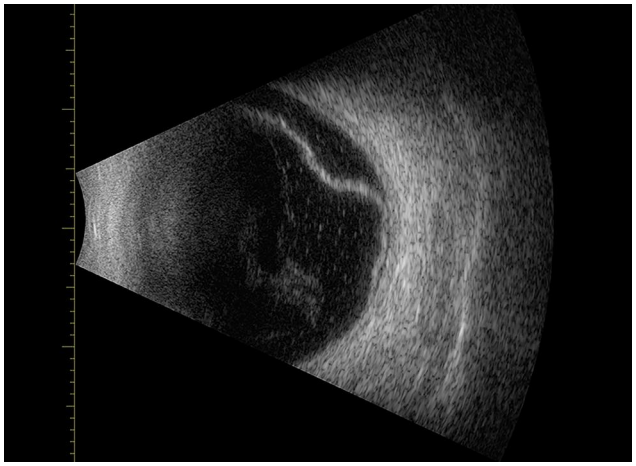

Figure 1 Example of retinal detachment seen on ocular ultrasound.

devices); (3) no history of eye diseases; and (4) no history of mental or nervous system diseases.

Parameters for MRI

Participants in the study were scanned with a Trio 3-Tesla MRI scanner, which required them to be quiet and maintain closed eyes. To obtain the structure image, we used the parameters to modulate the metamorphic gradient echo sequence. Then, the 3D metamorphic gradient echo pulse sequence was used to obtain the needed functional image. The specific parameters are shown in Table 1.

fMRI Data Analysis

In this study, we analyzed the above functional images. First, we used the MRIcro software to delete and classify the incomplete function data. In addition, to obtain balanced measurement signals, we deleted the first 10 volumes for each participant. Then, we used DPARSFA 4.0 software and SPM8 to pre-filter the data. After inputting the data into the Digital Image Communications system, the images were smoothed with the $3 \times 3 \times 3$ mm^3 full-width of 6 mm. Subsequently, we corrected the head motion and excluded the individuals whose head moved more than 1.5 mm to the x-, y-, or z-axes and whose angle range exceeded 1.5 mm.[13] A linear regression method was used to remove false variables from other sources.[14] Finally, we used the echo plane image template to standardize the fMRI images to satisfy the MNI space criteria.

We innovatively used the PerAF method to process fMRI data. Compared with ALFF, ReHo, and DC, PerAF is a more reliable and direct method based on rs-fMRI of voxel brain activity. PerAF can detect the changes and differences in specific brain regions in patients with RD and HCs. By measuring the percentage of BOLD signal strengths relative to the average BOLD signal intensity at each time point and obtaining the average value for the whole time series, the PerAF value was obtained. The PerAF value of each voxel was calculated as follows:

$$PerAF = \frac{1}{n}\sum_{i=1}^{n}\left|\frac{x_i - \mu}{\mu}\right| \times 100\% \quad (1)$$

$$\mu = \frac{1}{n}\sum_{i=1}^{n} x_i \quad (2)$$

where x_i represents the signal intensity of the i_{th} time point, n refers to the total number of time points in the time series, and μ represents the mean value of the time series.

Correlation Analysis

All RD patients who participated in this study were assessed with the Hospital Anxiety and Depression Scale (HADS),

Table 1 Information About MRI Parameters

Data Acquisition	Metamorphic Gradient Echo Sequence	3D Metamorphic Gradient Echo Pulse Sequence
Patient		
Sex		
Male	9	9
Female	6	6
Age, average range	48.63±12.16	49.69±12.36
Scan parameters		
Repetition time/echo time	1900/2.26 ms	2000/30 ms
Thickness/gap	1.0/0.5 mm	4.0/1.2 mm
Acquisition matrix	256×256	64×64
Field of view	250×250 mm	220×220 mm
Flip angle	90°	90°

Abbreviation: MRI, magnetic resonance imaging.

and the anxiety score (AS) and depression score (DS) for each patient were obtained. Pearson's correlation analysis was used to evaluate the correlation between HADS and PerAF values in the left inferior temporal gyrus, and the results were statistically significant at $P < 0.05$. We also used SPSS 24.0 software to analyze the data and produce a linear correlation graph.

Statistical Analysis

We used statistical software (SPSS 20.0; SPSS, Chicago, IL) to conduct an independent sample *t*-test and compare the differences between the two groups. The results were considered statistically significant at $P < 0.05$. The differences in PerAF values between the two groups were assessed with two-sample *t*-tests using the SPM8 toolkit ($P < 0.005$ for multiple comparisons using Gaussian Random Field theory. AlphaSim corrected at cluster > 40 voxels). Finally, ROC curve analysis was used to determine the average values of PerAF in specific brain regions of the RD and HC groups. Pearson's correlation analysis was used to evaluate the correlation between the specific brain regions of RD patients and their clinical characteristics and manifestations.

Results

Demographics and Visual Measurements

As shown in Table 2, the mean age of patients in the RD group was 48.63 ± 12.16 years old, and the mean weight was 57.64 ± 5.43 kg. The mean age of the HC group was 49.69 ± 12.36 years old and the mean weight was 56.63 ± 5.54 kg. We found that there were no significant differences in gender ($P > 0.99$), age ($P = 0.912$), or weight ($P = 0.821$) between the RD and HC groups. All participants in this study were right-handed. The best-corrected VA-left ($P = 0.017$) and best-corrected VA-right ($P = 0.012$) were significantly different. The mean duration of RD was 18.13 ± 7.75 days.

PerAF Differences

The PerAF signal values of the right fusiform gyrus and the left inferior temporal gyrus [Brodmann area (BA) 20] of RD patients were significantly higher than those of the HCs ($P < 0.001$). Details are shown in Figure 2A and B, and Table 3. As shown in Figure 2C, the mean altered PerAF values in the left inferior temporal gyrus and the right fusiform gyrus of the brain regions of RD and HC groups.

ROC Curve Analysis

ROC curve analysis was used to determine the average value of PerAF in different brain regions of the RD and HC groups. The results showed that there was a difference in the PerAF values between the RD and HC groups, which could be used as a potential diagnostic index. In our study, the AUC value of the right fusiform gyrus was 0.960 ($P < 0.001$; 95% CI: 0.900−1.000), and the AUC value of the left inferior temporal gyrus was 0.947 ($P < 0.001$; 95% CI: 0.874−1.000; Figure 3).

Correlation Analysis

A linear correlation analysis showed that the AS ($r = 0.885$, $P < 0.001$)/DS ($r = 0.756$, $P < 0.001$) of the HADS questionnaire and the duration ($r = 0.880$, $P < 0.001$) were positively correlated with the PerAF value of the left inferior temporal gyrus (Figure 4).

Discussion

PerAF is a new and more reliable processing method than ALFF, ReHo, and DC. It can also reduce the influence of the BOLD signal strength. In this experiment, we first used the PerAF method to study neural activity and its changes in different brain regions of patients with RD. The final results showed that the PerAF values of the right fusiform gyrus and the left inferior temporal gyrus were significantly higher than those of the HCs (see Figure 5 for details).

Table 2 The Conditions of Participants Included in the Study

Condition	RD	HCs	t value	P value*
Male/female	9/6	9/6	N/A	>0.99
Age (years)	48.63±12.16	49.69±12.36	−0.964	0.912
Weight (kg)	57.64±5.43	56.63±5.54	−0.889	0.821
Handedness	15R	15R	N/A	>0.99
Best-corrected VA-R	0.20±0.05	1.05±0.15	2.727	0.017
Best-corrected VA-L	0.15±0.05	1.05±0.20	2.946	0.012
Duration of RD (days)	18.13±7.75	N/A	N/A	N/A

Note: *P <0.05 Independent *t*-tests comparing two groups.
Abbreviations: RD, retinal detachment; HCs, healthy controls; L, left; R, right; N/A, not applicable; VA, visual acuity.

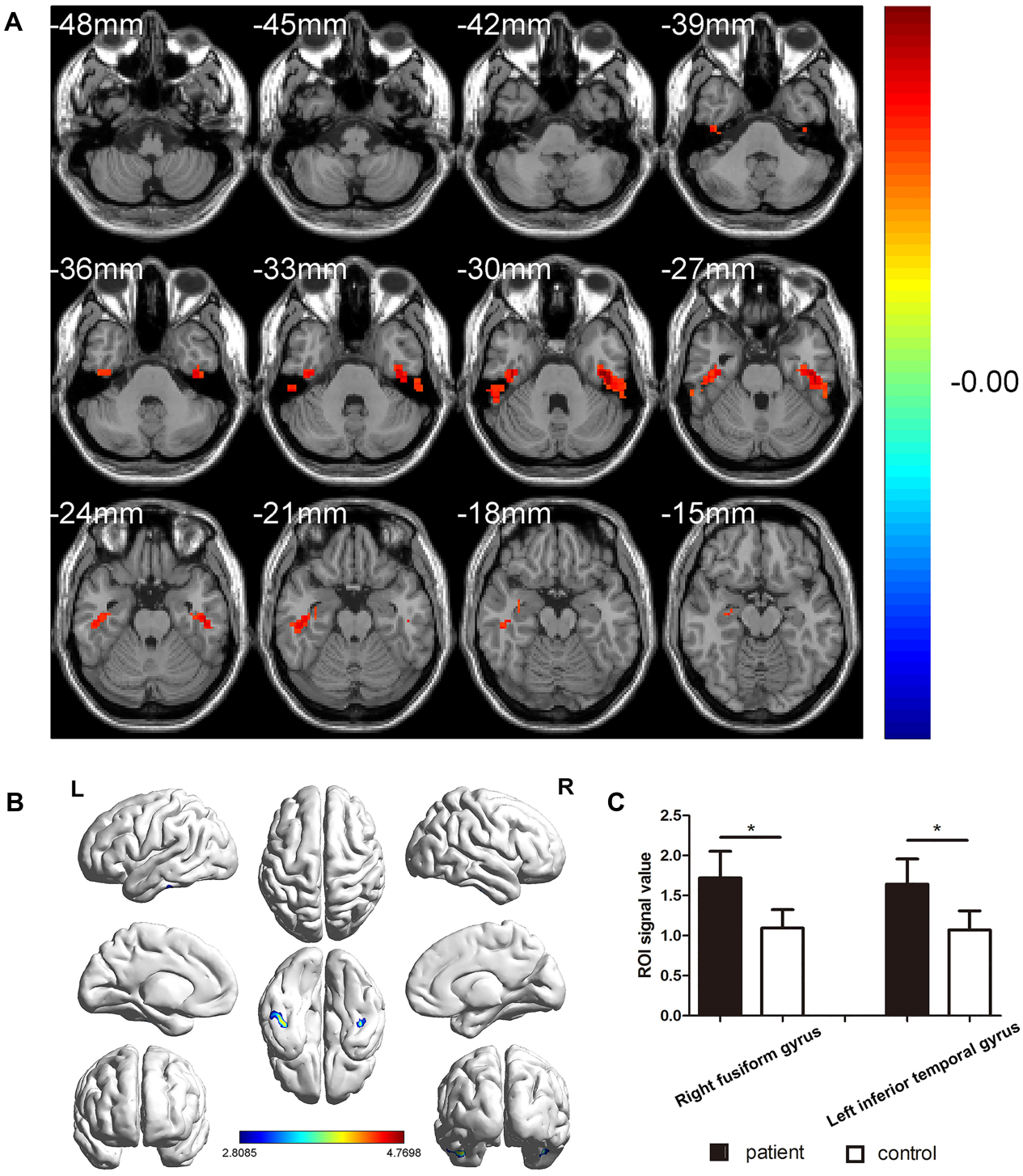

Figure 2 (**A** and **B**) Spontaneous brain activity in RD and HC groups. Red, blue and yellow shadows represent the strength of the signals. The right fusiform gyrus and left inferior temporal gyrus exhibit higher signals (P<0.005 for multiple comparisons using Gaussian random field theory, cluster >99 voxels, AlphaSim corrected). (**C**) The mean PerAF signal value between the RD and HC groups.
Note: Compared with HCs, asterisk means the statistical significance P < 0.05.
Abbreviations: RD, retinal detachment; HC, healthy control; PerAF, percent amplitude of fluctuation; R, right; L, left.

Some studies have shown that the fusiform gyrus is the key structure of powerful advanced visual computing. Its functions involve face recognition, object recognition, and reading, and are closely related to memory, multi-sensory integration, and perceptual function.[15] Through analysis of the functional neuroimaging results of young and old

Table 3 Brain Areas with Significantly Different PerAF Values Between the RD and HCs

Brain Areas	MNI Coordinates			BA	Number of Voxels	T value
	X	Y	Z			
Patient>HC						
Right Fusiform Gyrus	42	−18	−30	56	123	4.2751
Left Inferior Temporal	−42	−18	−30	89	123	4.7698

Note: The statistical threshold was set at a voxel level with P<0.005 for multiple comparisons using Gaussian random field theory (AlphaSim corrected at cluster >99 voxels, p<0.05).
Abbreviations: PerAF, percent amplitude of fluctuation; RD, retinal detachment; BA, Brodmann area; HC, healthy control; MNI, Montreal Neurological Institute.

people, it was determined that when a language task increased, the corresponding areas of the right hemisphere showed greater activation.[16] The function of the fusiform gyrus in face recognition and object secondary classification recognition is better in the right hemisphere than in the left hemisphere.[17] The face recognition area is located in the fusiform gyrus, which is a key brain area related to the skill of obtaining similar objects. Damage in this area can cause facial agnosia. Electrical brain stimulation of the right fusiform gyrus will distort facial vision, while electrical brain stimulation of the left fusiform gyrus will cause nonspecific visual changes.[18] Many scholars have suggested that independent neural mechanisms of the ventral visual cortex of the two hemispheres support the function of face and word recognition, respectively, so damage to both sides of the region does not affect function of the contralateral brain region. However, after studying patients with fusiform gyrus injury, it was determined that they not only suffer from poor facial recognition but also have some degree of problems with word recognition.[19] Words and the face may share the same neural processing, which is the result of the selective response of discrete neural regions to specific types of visual information.[20] Some scholars have suggested that different nodes in the face selection region of the fusiform gyrus produce different facial perception results, and when specific parts of this network area are damaged, corresponding facial distortion is observed.[21] An fMRI study showed that, in medial temporal lobe epilepsy (MTLE) patients with normal recognition ability, bilateral parahippocampal area/fusiform gyrus (PH/FG) had compensatory enhancement, which enabled patients to maintain recognition ability. Therefore, when the sensory and memory system was damaged, the nonspecific attention network might have been activated alternately.[22]

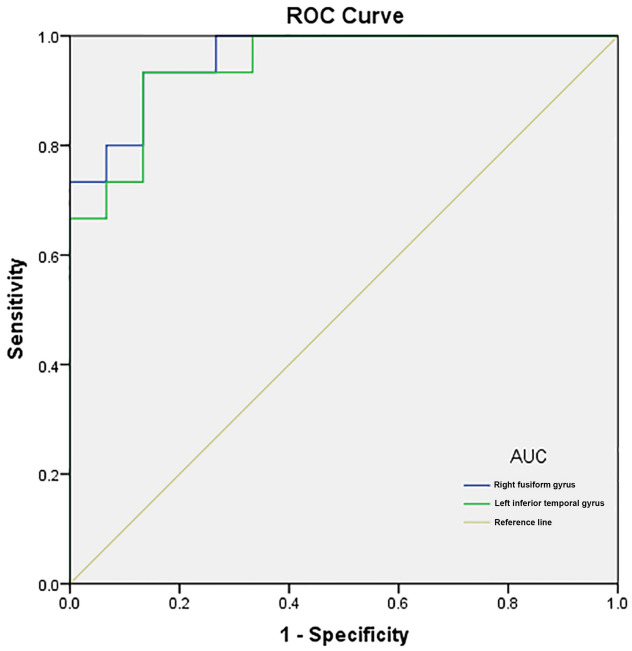

Figure 3 ROC curve analysis of the PerAF values for altered brain regions.
Notes: ROC curve analysis of the PerAF values for altered brain regions. The area under the ROC curve was 0.960, (P<0.001; 95% CI: 0.900–1.000) for the right fusiform gyrus, and 0.947 (P<0.001; 95% CI: 0.874–1.000) for left inferior temporal gyrus.
Abbreviations: ROC, receiver operating characteristic; PerAF, percent amplitude of fluctuation; AUC, area under the curve.

Based on the above analysis and discussion, combined with this study, the PerAF values of the right fusiform gyrus in RD patients were significantly higher than those in HCs. We speculate that this is the impairment of sensory system in patients with RD. when memory, multi-organ integration and perception tasks are increased, in order to enable patients to maintain recognition ability, which leads to compensatory increase of fusiform gyrus activation (Figure 6).

The ITG is a component of the dorsal visual pathway, involving high cognitive function, vision, language understanding, and emotion regulation.[23] Active maintenance of visual information is supported by activation of object representation in the subtemporal cortex.[24] The ITG participates in high-level visual processing and classification,

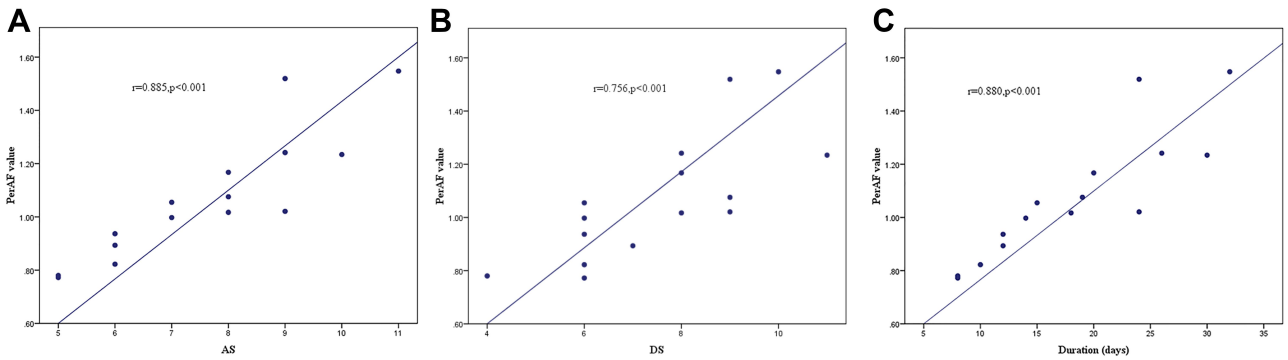

Figure 4 (**A**) Correlations between the anxiety scores of HADS and PerAF signal values in RD patients. (**B**) Correlations between the depression scores of HADS and PerAF signal values in RD patients. (**C**) Correlations between the durations of HADS and PerAF signal values in RD patients. The figure shows the anxiety and depression scores of HADS and the durations in RD patients were positively correlated with the PerAF values of left inferior temporal gyrus.
Abbreviations: AS, anxiety score; DS, depression score; HADS, Hospital Anxiety and Depression Scale; PerAF, percent amplitude of fluctuation; RD, retinal detachment.

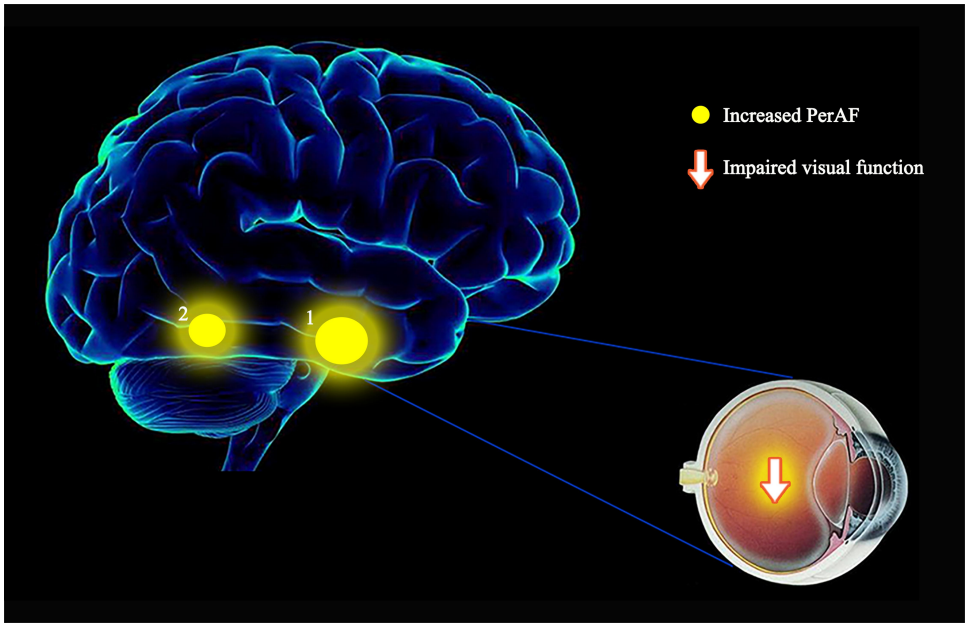

Figure 5 The mean PerAF values of altered brain regions. Compared with the HCs, the PerAF values of the following regions were increased to various extents: 1 – Left Inferior Temporal Gyrus (BA 89, t = 4.7698), 2 – Right Fusiform Gyrus (BA 56, t = 7.0916)).
Abbreviations: PerAF, percent amplitude of fluctuation; HCs, healthy controls; BA, Brodmann's area.

especially in the analysis of observed shapes.[25] When positron emission technology was used to analyze the semantic processing of words, the ITG showed obvious activation.[26] Correspondingly, when the ITG is damaged in patients with aphasia, there are often semantic defects,[27] and some studies have observed ITG atrophy in semantic dementia,[28] which supports their participation in semantic language understanding. Through meta-analysis connectivity research of the ITG, it was found that, although the ITG participates in language processing, it cannot be considered as the core language processing area, and it can be understood as a kind of language processing edge area.[29] Some studies have analyzed patients with depression with voxel level resting-state functional connectivity neuroimaging and found that FC in the inferior temporal gyrus is relatively reduced.[30] In addition, ITG dysfunction may be associated with eye diseases, such as primary open-angle glaucoma.[31]

We found that the PerAF values in the left inferior temporal gyrus of RD patients were significantly higher than those of HCs, suggesting that the functional activity of related brain regions was active. Because the category effect of the dorsal visual pathway is dominated by the top-down mechanism, but at the same time, it is the

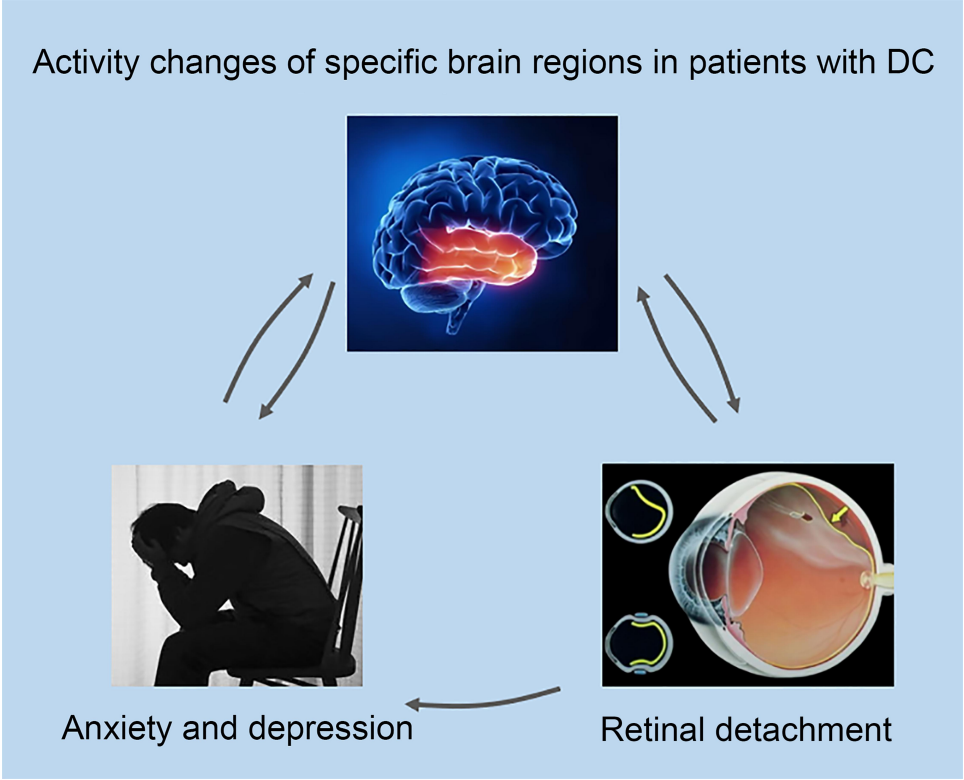

Figure 6 The relationship between retinal detachment, brain activity, and mood changes.

result of the dual mechanism that is regulated by the bottom-up mechanism.[23] We speculate that this may be due to abnormalities in the visual information transmission pathway in patients with RD, leading to dysfunction or overactivation of the dorsal visual pathway. This may provide some basis for cognitive function and visual impairment in patients with RD. In addition, we also found that the anxiety and depression scores of HADS and the durations in RD patients were positively correlated with the PerAF values of the left inferior temporal gyrus. That is to say, the higher the PerAF value of the left inferior temporal gyrus, the more likely to have anxiety and depression in patients with RD, and the duration will also be prolonged.

Conclusion

To sum up, we innovatively used the PerAF method to study changes in neural activity and brain function in brain regions of patients with RD. We found that the PerAF signal values of the left inferior temporal gyrus [Brodmann area (BA) 20] and the right fusiform gyrus of RD patients were significantly higher than those of HCs. These changes may increase the risk of corresponding brain dysfunction related diseases (Table 4). There were limitations in this study, such as the small study population and the wide range of population inclusion. As a new and reliable method, PerAF has great potential in voxel whole-brain analysis. Its value is helpful to predict the development and prognosis of RD patients and plays an important

Table 4 Brain Region Alternation and Its Potential Impact

Brain Regions	Experimental Result	Brain Function	Anticipated Results
Right fusiform gyrus	RD>HC	Face recognition, object recognition, reading, memory, multi-sensory integration and perceptual function	Face agnosia, character agnosia, perceptual disorder, memory disorder and dyslexia
Left inferior temporal gyrus	RD>HC	High cognitive function, visual understanding, language understanding and emotion regulation	Visual comprehension disorders, visual processing and classification barriers, semantic defects

Abbreviations: RD, retinal detachment; HC, healthy control.

role in the early diagnosis of RD. In addition, the changes of nerve activity in specific brain regions of RD patients increase the risk of brain dysfunction related diseases, which is helpful to understand the pathological mechanism of vision decline or related diseases in RD patients.

Data Sharing Statement

The data related to this experiment can be obtained from the corresponding author.

Ethics Approval and Consent to Participate

This research method followed the Helsinki Declaration and was approved by the medical ethics committee of the First Affiliated Hospital of Nanchang University. Participants maintained a voluntary and positive attitude towards the study. After knowing the purpose, procedure, and risks of the study, they willingly cooperated and signed the informed consent form.

Acknowledgments

We thank the participants for their help and wish them a speedy recovery.

Funding

This study was supported by the Key Research Foundation of Jiangxi Province (No: 20181BBG70004); Excellent Talents Development Project of jiangxi Province (No: 20192BCBL23020); Natural Science Foundation of jiangxi Province (No: 20181BAB205034); Grassroots Health Appropriate Technology "Spark Promotion Plan" Project of Jiangxi Province (No: 20188003); Health Development Planning Commission Science Foundation of Jiangxi Province (No: 20175116, 20201032); Health Development Planning Commission Science TCM Foundation of Jiangxi Province (No: 2018A060).

Disclosure

The authors declare that they have no competing interests.

References

1. Steel D. Retinal detachment. *BMJ Clin Evid*. 2014;0710:2014.
2. Lai CT, Kung WH, Lin CJ, et al. Outcome of primary rhegmatogenous retinal detachment using microincision vitrectomy and sutureless wide-angle viewing systems. *BMC Ophthalmol*. 2019;19(1):230. doi:10.1186/s12886-019-1238-3
3. Vuković D, Pajić SP, Paović P. Retinal detachment in the eye with the choroidal coloboma. *Srp Arh Celok Lek*. 2014;142(11–12):717–720. doi:10.2298/SARH1412717V
4. Feltgen N, Walter P. Rhegmatogenous retinal detachment–an ophthalmologic emergency. *Dtsch Arztebl Int*. 2014;111(1–2):12–22. doi:10.3238/arztebl.2014.0012
5. Han KJ, Lee YH, Vavvas DG. Optical coherence tomography automated layer segmentation of macula after retinal detachment repair. *PLoS One*. 2018;13(5):e0197058. doi:10.1371/journal.pone.0197058
6. Gottlieb M, Holladay D, Peksa GD, Carpenter CR. Point-of-care ocular ultrasound for the diagnosis of retinal detachment: a systematic review and meta-analysis. *Acad Emerg Med*. 2019;26(8):931–939. doi:10.1111/acem.13682
7. Grozdanic SD, Lazic T, Kecova H, et al. Optical coherence tomography and molecular analysis of sudden acquired retinal degeneration syndrome (SARDS) eyes suggests the immune-mediated nature of retinal damage. *Vet Ophthalmol*. 2019;22(3):305–327. doi:10.1111/vop.12597
8. Kesavadas C. Resting state functional magnetic resonance imaging: an emerging clinical tool. *Neurol India*. 2013;61(2):103–104. doi:10.4103/0028-3886.111107
9. Smitha KA, Akhil Raja K, Arun KM, et al. Resting state fMRI: a review on methods in resting state connectivity analysis and resting state networks. *Neuroradiol*. 2017;30(4):305–317. doi:10.1177/1971400917697342
10. Lin WC, Hsu TW, Chen CL, et al. Resting state-fMRI with ReHo analysis as a non-invasive modality for the prognosis of cirrhotic patients with overt hepatic encephalopathy. *PLoS One*. 2015;10(5):e0126834. doi:10.1371/journal.pone.0126834
11. Zhao N, Yuan LX, Jia XZ, et al. Intra- and inter-scanner reliability of voxel-wise whole-brain analytic metrics for resting state fMRI. *Front Neuroinform*. 2018;12:54. doi:10.3389/fninf.2018.00054
12. Jia XZ, Sun JW, Ji GJ, et al. Percent amplitude of fluctuation: a simple measure for resting-state fMRI signal at single voxel level. *PLoS One*. 2020;15(1):e0227021. doi:10.1371/journal.pone.0227021
13. Liu X, Yan Z, Wang T, et al. Connectivity pattern differences bilaterally in the cerebellum posterior lobe in healthy subjects after normal sleep and sleep deprivation: a resting-state functional MRI study. *Neuropsychiatr Dis Treat*. 2015;11:1279–1289. doi:10.2147/NDT.S84204
14. Fox MD, Snyder AZ, Vincent JL, et al. The human brain is intrinsically organized into dynamic, anticorrelated functional networks. *Proc Natl Acad Sci USA*. 2005;102(27):9673–9678. doi:10.1073/pnas.0504136102
15. Weiner KS, Zilles K. The anatomical and functional specialization of the fusiform gyrus. *Neuropsychologia*. 2016;83:48–62. doi:10.1016/j.neuropsychologia.2015.06.033
16. Hoffman P, Morcom AM. Age-related changes in the neural networks supporting semantic cognition: a meta-analysis of 47 functional neuroimaging studies. *Neurosci Biobehav Rev*. 2018;84:134–150. doi:10.1016/j.neubiorev.2017.11.010
17. Keller CJ, Davidesco I, Megevand P, et al. Tuning face perception with electrical stimulation of the fusiform gyrus. *Hum Brain Mapp*. 2017;38(6):2830–2842. doi:10.1002/hbm.23543
18. Rangarajan V, Hermes D, Foster BL, et al. Electrical stimulation of the left and right human fusiform gyrus causes different effects in conscious face perception. *J Neurosci*. 2014;34(38):12828–12836. doi:10.1523/JNEUROSCI.0527-14.2014
19. Behrmann M, Plaut DC. Bilateral hemispheric processing of words and faces: evidence from word impairments in prosopagnosia and face impairments in pure alexia. *Cereb Cortex*. 2014;24(4):1102–1118. doi:10.1093/cercor/bhs390
20. Harris RJ, Rice GE, Young AW, et al. Distinct but overlapping patterns of response to words and faces in the fusiform gyrus. *Cereb Cortex*. 2016;26(7):3161–3168. doi:10.1093/cercor/bhv147
21. Rossion B. Constraining the cortical face network by neuroimaging studies of acquired prosopagnosia. *Neuroimage*. 2008;40(2):423–426. doi:10.1016/j.neuroimage.2007.10.047

22. Guedj E, Bettus G, Barbeau EJ, et al. Hyperactivation of parahippocampal region and fusiform gyrus associated with successful encoding in medial temporal lobe epilepsy. *Epilepsia*. 2011;52(6):1100–1109. doi:10.1111/j.1528-1167.2011.03052.x
23. Lin YH, Young IM, Conner AK. Anatomy and white matter connections of the inferior temporal gyrus. *World Neurosurg*. 2020;143:e656–e666. doi:10.1016/j.wneu.2020.08.058
24. Ranganath C, Cohen MX, Dam C, et al. Inferior temporal, prefrontal, and hippocampal contributions to visual working memory maintenance and associative memory retrieval. *J Neurosci*. 2004;24(16):3917–3925. doi:10.1523/JNEUROSCI.5053-03.2004
25. Freedman DJ, Riesenhuber M, Poggio T, et al. A comparison of primate prefrontal and inferior temporal cortices during visual categorization. *J Neurosci*. 2003;23(12):5235–5246. doi:10.1523/JNEUROSCI.23-12-05235.2003
26. Démonet JF, Chollet F, Ramsay S, et al. The anatomy of phonological and semantic processing in normal subjects. *Brain*. 1992;115(6):1753–1768. doi:10.1093/brain/115.6.1753
27. Gao W, Sun X, Xie H, et al. The regional neuronal activity in left posterior middle temporal gyrus is correlated with the severity of chronic aphasia. *Neuropsychiatr Dis Treat*. 2017;13:1937–1945.
28. Mummery CJ, Patterson K, Price CJ, et al. A voxel-based morphometry study of semantic dementia: relationship between temporal lobe atrophy and semantic memory. *Ann Neurol*. 2000;47(1):36–45.
29. Ardila A, Bernal B, Rosselli M. How extended is wernicke's area? Meta-analytic connectivity study of BA20 and integrative proposal. *Neurosci J*. 2016;4962562:2016.
30. Cheng W, Rolls ET, Qiu J, et al. Functional connectivity of the human amygdala in health and in depression. *Soc Cogn Affect Neurosci*. 2018;13(6):557–568. doi:10.1093/scan/nsy032
31. Li C, Cai P, Shi L, et al. Voxel-based morphometry of the visual-related cortex in primary open angle glaucoma. *Curr Eye Res*. 2012;37(9):794–802. doi:10.3109/02713683.2012.683506